Measurement of silicon solar cells ac parameters

Viktor Schlosser[1] *and Ahmed Ghitas*[2]

[1]Institute for Material Physics,
Faculty of Physics, Vienna University, Strudlhofgasse 4,
A-1090 Vienna, Austria, E.mail: Viktor.Schlosser@univie.ac.at

[2]Solar Physics Laboratory,
National Research Institute of Astronomy and Geophysics,
(NRIAG) Helwan, Cairo, Egypt, E.mail: Aghitas@hotmail.com

Abstract

Photovoltaic modules are operated as DC devices. But they exhibit a complex impedance due to the solar cell design. Subsequent electronic circuits for electric power conditioning are designed to match the input at standard operating conditions. During operation the real part as well as the imaginary part of the impedance of photovoltaic modules change due to ambient conditions such as illumination level and temperature. A mismatch due to changes of the complex impedance can lead to a reduced performance of the whole power generating system. Hence, for designing such efficient high power photovoltaic systems a detailed study on AC parameters of solar cells are important. In terrestrial applications, the solar cell is exposed to temperatures varying from 10°C to 50°C. Therefore, to study the potential effect of temperature on system performance, the AC parameters (cell capacitance and cell conductance) of silicon solar cells are determined at different temperatures using AC small signal measurement techniques. The cell transition capacitance and the cell conductance are calculated from small signal impedance measurements under dark condition. It is observed that the solar cell capacitance increases whereas the real part of cell impedance decreases with temperature increasing. From these measurements the temperature dependence of the complex impedance under power generating condition was estimated. In addition the solar cell's capacitance at various operating conditions was derived from transient measurements under illumination. Within error limits these results confirmed the estimated variation of the complex impedance with temperature.

Keywords: Silicon solar cell; AC parameters; Temperature; Capacitance; Resistance

Introduction

Renewable energies are being more popular and viewed in some cases as a viable alternative to conventional sources of energy. Photovoltaic power generation has become a very important non-conventional energy source. The technology of photovoltaics has evolved and matured to become an economical alternative to other power sources. The demand for high power and high efficiency has necessitated the use of high-speed switching charge controllers for solar array power conditioners. To design an efficient and reliable switching charge controller, the AC parameters of solar cells (especially the cell capacitance and cell conductance) has need to be investigated. (Deshmukh et al, 2004, 2005).

When the solar panel is operating under the outdoor condition, the variation in the temperature for a given operating voltage will vary the cell or panel operating condition

(voltage and current) and thus it's AC parameters. The AC parameters of a high efficient commercial solar cell were measured at different cell temperatures by varying the cell bias voltage (forward and reverse) under dark condition using impedance spectroscopy technique. It was found that the cell capacitance increases with temperature where the cell resistance decreases, at any bias voltage (Anil Kumara et al, 2000, 2001, 2005).

In high power solar charging systems, the load is permanently connected to the system and draws power continuously from it. Hence, the solar panels need to supply continuous power to maintain the battery in optimally charged state, in order to provide the required amount of power to the load. Due to this, the solar cell or panel is required to be switched between battery and the shunt switch (shorting the solar panel) rapidly. A solar cell can be modelled as a parallel RC network with a series resistance. Due to the capacitance present in the solar cell, high voltage of solar array (across capacitance) gets discharged through shunt switch, present in PV system as a part of the charge controller, causing significant power loss P, which is given by (Liu et al, 1990)

$$P = \frac{1}{2} C V^2 f \tag{1}$$

where, C is the solar array capacitance, V is the bus voltage and f is the frequency of the charge controller. Therefore, AC parameters, in particular, the solar cell capacitance is an important parameter in the design of fast acting and reliable charge controllers. The solar cell capacitance equals the connection of (i) a transition capacitance C_T and (ii) a diffusion capacitance C_d in parallel.

The transition capacitance or depletion capacitance is for an one sided abrupt pn-junction profile given by (Millman and Halkias, 1972)

$$C_T = A\sqrt{\frac{qN_B \varepsilon \varepsilon_o}{2(V_0 - V_d)}} \tag{2}$$

where, A is the area of solar cell, q is the electron charge, 1.602×10^{-19} C, N_B is the doping concentration in the base region, ε_o is the permittivity of free space, 8.85×10^{-12} F/m, ε is the permittivity of the semiconductor material (for Si, $\varepsilon = 11.7$), V_0 is the built in voltage and V_d the applied voltage.

Assuming that the diode current is governed by diffusion the diffusion capacitance C_d can be expressed by (Sze, 1985)

$$C_d = \frac{\tau G}{2} = \frac{\tau}{2}\frac{dI}{dV_d} \tag{3}$$

where, G is the diode incremental conductance, and τ the effective minority carrier lifetime in the base region of the pn-junction. G can be obtained from the first derivation of static I-V

measurements or from low frequency small signal AC measurements ($\omega\tau<<1$). The effective minority carrier lifetime τ is calculated as follows (Mahan et al, 1979):

$$\tau = \frac{\eta kT}{q}\frac{1}{(\mathrm{d}V_{\mathrm{OC}}/\mathrm{d}t)} = \frac{\eta V_{\mathrm{T}}}{(\mathrm{d}V_{\mathrm{OC}}/\mathrm{d}t)} \tag{4}$$

where, η is the ideality factor, k is the Boltzman's constant, 8.617×10^{-5} eV/K, T is the absolute temperature in K, q is the electronic charge , $V_{\mathrm{T}} = kT/q$ is the thermal voltage and $\mathrm{d}V_{\mathrm{OC}}/\mathrm{d}t$ is the rate of linear voltage decay in V/s calculated from voltage decay. The solar cell resistance R_{P} is the parallel combination of the static R_{T} and dynamic resistance R_{d}. These resistances are calculated from *I-V* characteristics as follows:

The static resistance is given by (Millman and Halkias, 1972)

$$R_{\mathrm{T}} = \frac{V_d}{I} \tag{5}$$

The dynamic resistance R_{d} is given by

$$R_{\mathrm{d}} = \frac{1}{G} \tag{6}$$

The effective or parallel resistance (R_{P}) of the solar cell is given by

$$R_P^{-1} = R_T^{-1} + R_d^{-1} \tag{7}$$

Depending on V_{d} and the illumination level of the solar cell either C_{T} or C_{d} dominates the total capacitance. For reverse bias voltages under dark condition C_{d} which is mainly caused by the diffusion of free carriers is negligible. Once V_{d} exceeds V_0 the cell capacitance is merely described by C_{d}. In the regime where a solar cell is operated for power conversion ($0<V_{\mathrm{d}}<V_0$) both capacitors contribute to the total capacitance. For crystalline silicon solar cells the recombination loss current can contribute or even dominate the total diode current of the device depending on the incident light intensity. Therefore care has to be taken when the above equations which were evaluated for the case of a mere diffusion current are applied to derive solar cell parameters.

In the present work the changes of the solar cell's AC impedance with temperature was investigated in order to estimate the magnitude of the introduced deviation from the standard operation.

Experimentation

The experimental investigations were carried out on a photovoltaic solar cell made from high purity silicon. The silicon solar cell was manufactured by Solartec (Czech Republic) and of type SC14-12. The area A was $51.45\times17.1\mathrm{mm}^2$ The optical cell properties are determined firstly. From reflectance measurements the thickness, d_{AR} of the antireflection coating

material consisting of Si_3N_4 was determined. As shown in Fig.1 the coating material thickness value was found to be 188 nm. This is much thicker than necessary for a single layer antireflection coating which has to fulfil the criteria $nd_{AR}=\lambda/4$. Where n is the index of refraction which for Si_3N_4 is about 2 and λ is the wavelength for minimal reflectance which for c-Si solar cells is typically chosen around 600 nm (See dotted curve in Fig.1). This suggests that the layer's thickness was adjusted to satisfy rather visual effects. Although absorption in the layer still remains negligible but an enhanced reflection in the IR wavelength region occur. Therefore a somewhat reduced power output of the solar cell has to be expected. The fully metallised backside of the cell was put on a heat able copper plate with a thin liquid Ga/In solder in between to ensure high electrical and thermal connection. The front metal busbar was electrically connected with a spring contact. A Pt100 resistor mounted beside the cell on the copper plate served as temperature sensor.

The spectral response was measured at room temperature. The observed quantum efficiency in the long wavelength region is exclusively governed by the cell's thickness which was specified by the manufacturer to be 320±50 µm and not by the minority carrier diffusion length, L_n.

In the dark current voltage measurements of the cell operated in DC mode were taken in the temperature range between 295 K and 340 K. The recorded data pairs were fitted using a two diode model – diffusion, I_{dif} and recombination, I_{rec} current – with respect of ohmic contributions expressed by a series resistance, R_S and a shunt conductance, $G_{SH} = 1/R_d$. Where R_S is temperature independent $(2.1\pm0.3)\Omega cm^2$ due to the non-permanent contacts to the external circuit. Both saturation current densities, $j_{0rec} = I_{0rec}/A$ for the recombination current and j_{0dif} for the diffusion current obey an activation law as can be seen in the Arhenius plot of Fig.2. The dependencies are in agreement with theory which predict that j_{0dif} varies with n_i^2 and j_{0rec} varies with n_i once all dopants are ionised.

With an assumption that the effective mass of carrier does not change with temperature, n_i can be written as $n_i^2 = C\,T^3 \exp(-E_G/kT)$ (Kano, 1998). Where n_i is the intrinsic carrier concentration of electron-hole pair in the base semiconductor of the solar cell material, C is the constant, E_G is the band gap energy in eV. In Fig.3 the temperature dependence of the shunt conductance G_{SH} derived from the DC measurements is plotted together with the results of the differential conductance G_{AC} obtained from small signal AC measurements made at a frequency of 10 kHz. The scaling of both axis in Fig.3 is the same but the offset differs by 0.726 mS. Except of this offset both measurements show the same temperature dependence of the conductance which indicate that in the case of the small signal measurements a temperature independent contribution $G(f)$ is present which mostly is observed once the cell's

surface is exposed to air. It is explained by creep currents on the surface and varies with the measurement frequency. The experimental set up for the small signal impedance measurements under dark condition is shown in Fig.4.

The generator output of a dual phase lock in amplifier (Model 830 from Stanford Research) generates a sine wave of 30 mV_{eff} which is superimposed with a DC Voltage coming from a ground free voltage source (Model 230 from Keithley Instruments) The mixed signal is applied to the device under test, DUT (solar cell) connected in series with a precise ohmic resistor R_I of known value which serves as a current monitor. The voltage signal at the resistor is fed to the input of the lock in amplifier which detects the AC component and to an A/D converter input which detects the DC component of the signal. From the AC component the lock in amplifier computes the magnitude and the phase relative to the output of the sine wave generator. It's frequency is adjustable between 1Hz and 100kHz. Both instruments are connected by a GPIB interface to a PC with installed LabWindows CVI software from National Instruments. All functions of the interfaced devices are computer controlled and the measured signals are transferred to the PC. From the knowledge of (i) the voltage (ii) the current and (iii) the phase the complex impedance of the DUT (device under test) can be calculated. Thus by varying the DC voltage of the reverse biased solar cell the transition capacitance C_T and the AC conductance can be recorded as a function of the voltage, C(V) and $G_{AC}(V)$. The results of AC conductance at zero bias voltage $G_{AC}(0)$ are shown in Fig.3. The transition capacitance is plotted as $1/C^2$ against the bias voltage (shown in Fig.5). According to the relation of C_T on V_d for an one sided abrupt planar pn-junction this relation should be linear (Equ.2). The two parameters N_B and V_0 can be evaluated by a linear fit of the measured data pairs as shown in Fig.5. In c-Si all shallow acceptors will be ionised above 250 K. Even in moderately low doped silicon the intrinsic carrier concentration is very low to contribute noticeably to the total carrier concentration below about 400 K. Therefore the observed temperature independent doping concentration of $N_B=5.7\times10^{16}$ cm^{-3} was expected. Since the base material of the solar cell was p-Si this concentration corresponds to a resistivity ρ of 0.5 Ωcm. The built in voltage decreases linearly with the temperature as can be seen in Fig.6. The slope was found to be –2.85 mVK^{-1}.

When the cell is operated as a photovoltaic current generator the cell is forward biased at voltages less than V_0. Therefore C_d contributes to the total observable capacitance. However the total capacitance still increases rapidly with increasing voltage. In order to examine the complex impedance of the solar cell under photovoltaic operation conditions the experimental set up which is schematically shown in Fig.7 was used. The cell was illuminated with 4 low voltage tungsten halogen lamps which were powered by a highly stabilised DC power supply.

The AC excitation of the solar cell was done by switching a 1W light emitting diode (Luxeon Star) on and off which leads to an additional light generated alternating current in the solar cell. The centre wavelength at maxim amplitude of the LED was 651 nm and the half bandwidth is 28 nm. It was switched at a frequency of 1kHz with a duty cycle of 50 per cent. The rise and fall time of the emitted intensity which was detected by the use of a 100 MHz avalanche photodiode was found to be better than 0.7 µs. The beam characteristics causes an inhomogeneous intensity distribution over the cell's surface although the whole cell was illuminated. Since we used a monocrystalline device of high purity silicon we assume, that this circumstance has no effect on the evaluated capacitance of the solar cell. The emitted intensity was adjusted to yield in a voltage signal of approximately 5mV measured with a digital storage oscilloscope at the beginning of the data recording and then left unchanged. Both, light intensity fluctuations from the background and electromagnetic distortion cause a high noise level at the electrical terminals of the solar cell. This inhibited the application of the previously used sensitive lock in detection technique. Instead the impedance was evaluated from the signal rise time observed with the 100 MHz oscilloscope (Hewlett Packard, model 54600B). Despite intense signal averaging the introduced noise causes rather high errors. Below an observed time constant of 1 µs the systematic error introduced by the rise time of the LED which is about 0.7 µs has to be considered. To ease data evaluation a very simple circuit was used as adjustable electronic load. It consists of a 1 Ω ohmic resistor, R_I which was used for the current determination in series with the drain source channel R_{DS} of a SIPMOS transistor (BUZ 100S). By controlling the gate voltage R_{DS} can be varied between 0.05 Ω and several MΩ. The gate voltage was set by the use of a precise voltage source (Model 230 from Keithley Instruments). The DC output of the cell determined from measurements of the current and the voltage with two digital voltmeters (Fluke 8840A and Keithley 199) was used as input to a feed back loop. Depending on the desired operating conditions the gate voltage of the transistor and thus R_{DS} were adjusted to maintain a pre set constant value of either the cell current, the cell voltage or the load resistance during a temperature sweep. All instruments were connected to the PC over the GPIB interface bus and controlled by the executed software based on LabWindows CVI. The temperature detected by the Pt100 element which was mounted on the copper plate beside the solar cell was simultaneously recorded by the same data acquisition program. It has to be mentioned that we have found some evidence (differences of the registered data occurred during heating and cooling the sample) that the temperature in the active region of the solar cell is not exactly the same as on it's backside which is in electrical and thermal contact with the copper

plate. The error introduced in the determination of the temperature was estimated to be less than 2 K.

Results and Discussion

The load which is powered by a photovoltaic current generator may be operated in two basic modes independent of changes of the ambient conditions, predominately the incident intensity but although the cell temperature.

1. At constant current or
2. At constant voltage.

In practice many systems are operated in a different way which can be considered to be a mixture or combination of these two basic modes. In very simple systems the load resistance often is kept fixed. Optimised systems use maximum power trackers to adjust the load to the point of maximum power output of the solar generator. In both cases the current as well as the voltage change with changing ambient conditions.

Since investigations of the influence of the cell's impedance on the temperature are more simple to discuss when it is operated in a basic mode, the experiment was carried out first under these two conditions. The load was adjusted to either maintain (i) a constant current or (ii) a constant voltage. Finally the load was kept constant and the experiment was repeated. In all cases the incident intensity was kept constant and the cell was heated from room temperature to above 340 K. The experimental conditions with respect to the solar cell's I(V) characteristic are illustrated in Fig.8. As can be seen the magnitude of the load resistance for all three modes is chosen for a power output which is close to the maximum power point indicated by MPP.

As known from the determination of the depletion capacitance in the dark the capacitance will increase with voltage and with temperature. The latter is due to the shift of the built in voltage towards lower values. Keeping the current constant lead to decreasing voltages with increasing temperature. Decreasing the voltage will decrease the capacitance, increasing the temperature will increase the capacitance. So it is expected that the both effects partly compensate each other resulting in a rather small change of the capacitance. Once the voltage is kept constant merely the temperature causes a change in the capacitance. This means that in this case the change will be significantly larger. The measured rise time τ_{rise} correlates with C and R. $\tau_{rise}=RC$ where R is the load resistance ($R = R_T-R_S$) and C the cell capacitance. The dependence of the load resistance on temperature was obtained from the DC measurements of the actual current and voltage and is plotted in Fig.9. In the case of a constant current of 0.110A it decreases linearly with temperature which agrees with the observed linear reduction of the open circuit voltage with temperature. In the case of a constant voltage which was

fixed to 0.405V the diode current losses, I_D increase with temperature obeying a thermal activation law as shown before. Therefore the cell's current $I(V) \propto I_L - I_D$ decreases non linear resulting in a strong increase of the resistance with temperature. I_L is the light generated current which is practically voltage independent for crystalline Si cells. This experimentally verified behaviour of the load resistance with temperature together with the knowledge of the transition capacitance and its temperature dependence allows to compute RC_T versus temperature in order to predict the magnitude of change with temperature for the different operating conditions. As can be seen in Fig.10 (right axis, full lines) *RC* increases 4 times when the temperature rises from 300 K to 350 K in the case that the cell is operated in the constant voltage mode. At a constant current a decrease of about 50 per cent is expected for the same temperature range. When the load resistance is kept constant at 4 Ω, *RC* is nearly independent of the temperature. The experimentally observed results are also plotted as symbols in Fig.10 and scaled by the left axis. Within the unsatisfactorily large error bars they are in good agreement with the calculations except that the capacitance derived from the measurements is somewhat reduced which was expected due to the contributions of C_d.

The case when the solar cell would have been operated at it's MPP appears to be similar to the case of constant current operation. It can be seen in Fig.8. that the MPP shifts mainly with the voltage and only little with the current.

Conclusions

Depending on the operation conditions the impedance of a solar cell are subjected to significant changes which not only are caused by changes of the incident light intensity but also by temperature variations as we have experimentally demonstrated. Although our experiments were restricted to a single photovoltaic cell, a module can be considered as a series and parallel connection of multiple cells and therefore a similar characteristic can be expected. Without the knowledge of the electronic circuitry of the connected electric load or power conditioning system it is not possible to estimate the consequences of a widely varying impedance. However the *RC* time constant of a solar power system determines the AC transfer characteristic and precautions will be necessary to avoid that unacceptable high noise levels are introduced to the connected power distribution system.

References

1. Anil Kumar R., Suresh M.S., Nagaraju J. (2000) Measurement and comparison of AC parameters of silicon (BSR and BSFR) and gallium arsenide (Ga/As/Ge) solar cells used in space applications, Solar Energy Materials & Solar Cells, 60, 155-166.

2. Anil Kumar R., Suresh M.S., Nagaraju J. (2001) Facility to measure solar cell ac parameters using an impedance spectroscopy technique, Review of Scientific Instruments, 72, 3422-3426.
3. Anil Kumar R., Suresh M.S., Nagaraju J. (2005) Silicon (BSFR) solar cell AC parameters at different temperatures, Solar Energy Materials & Solar Cells, 85, 397-406.
4. Deshmukh M.P., Anil Kumar R., Nagaraju J. (2004) Measurement of solar cell ac parameters using the time domain technique, Review of Scientific Instruments, 75 (8), 3422-3426.
5. Deshmukh, M.P. Nagaraju, J. (2005) Measurement of $CuInSe_2$ solar cell AC parameters, Solar Energy Materials & Solar Cells, 85: 407-413.
6. Deshmukh, M.P. Nagaraju, J. (2005) Measurement of silicon and GaAs/Ge solar cell device parameters, Solar Energy Materials & Solar Cells, 89: 403-408.
7. Kano K. (1998) Semiconductor Devices, Prentice-Hall, Englewood Cliff, NJ, 61–63.
8. Liu K.H., Lee F.C., (1990) Zero-voltage switching technique in DC/DC converters, IEEE Transactions on Power electronics, 5, 293-304.
9. Mahan J.E., Thomas W.E., Robert I.F., and Roy K. (1979) Measurement of Minority carrier lifetime in solar cells from photo-induced open circuit voltage decay, IEEE Trans. Electron. Devices. 26 (5): 733–739.
10. Millman, J., Halkias, C.C. (1972) Integrated Electronics: analog and digital circuits and systems, Tata McGraw Hill, New Delhi.
11. Sze S.M. (1985) Semiconductor Devices, John Wiley&Sons New York.

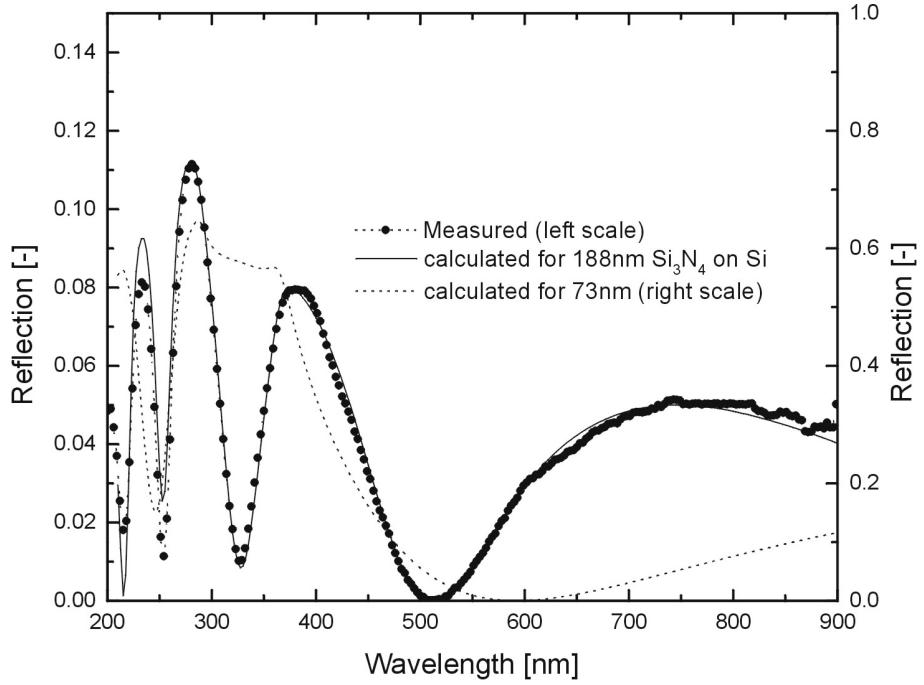

Figure 1. Measured and calculated reflectance of Si_3N_4 on silicon. The dashed curve show the reflectance for an optimised single layer antireflection coating with Si_3N_4. The calculations were done by using the program *FilmWizard*.

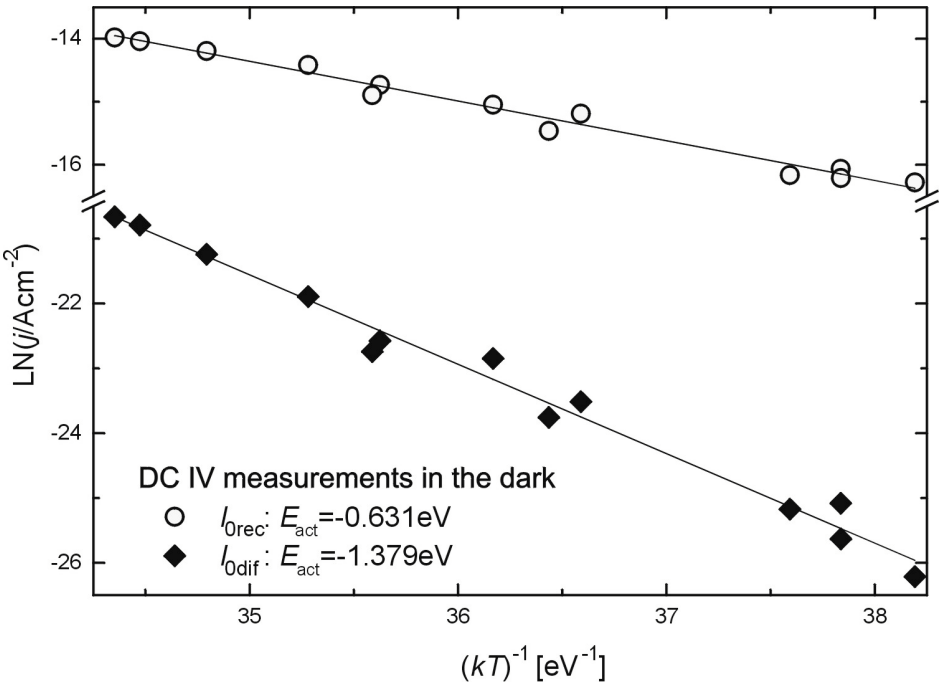

Figure 2. Arhenius plot of the saturation current densities derived from the I(V) characteristics under dark conditions. Both currents are thermally activated with different energies E_{act} derived from a linear fit.

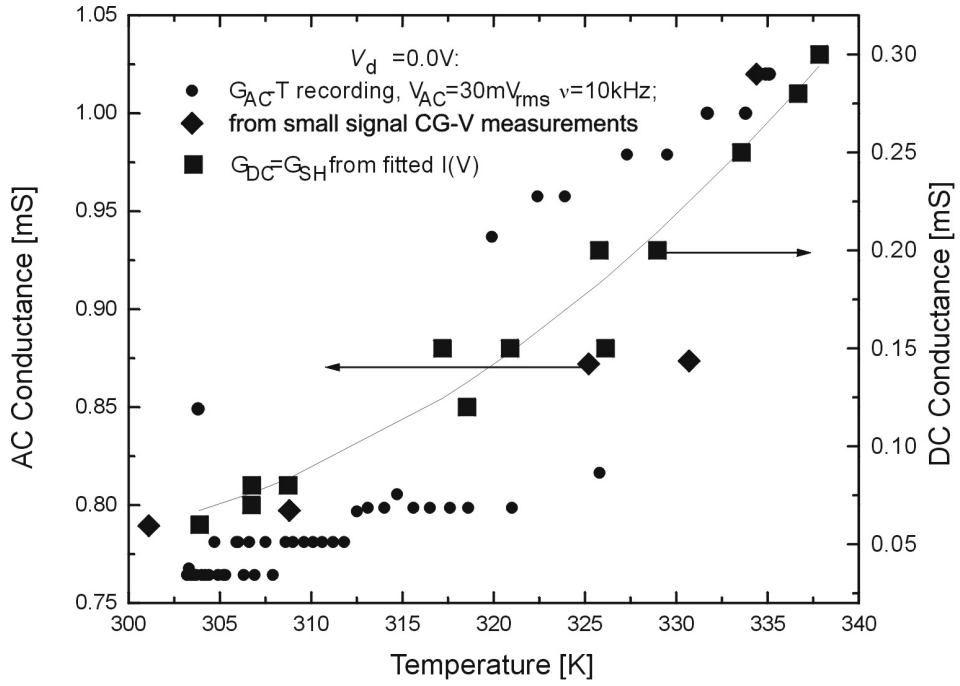

Figure 3. Comparison of the differential conductance G_{AC} (left axis) and G_{DC} (right axis). G_{AC} was derived from small signal impedance measurements and G_{DC} was found by the evaluation of the I(V) curves in the dark.

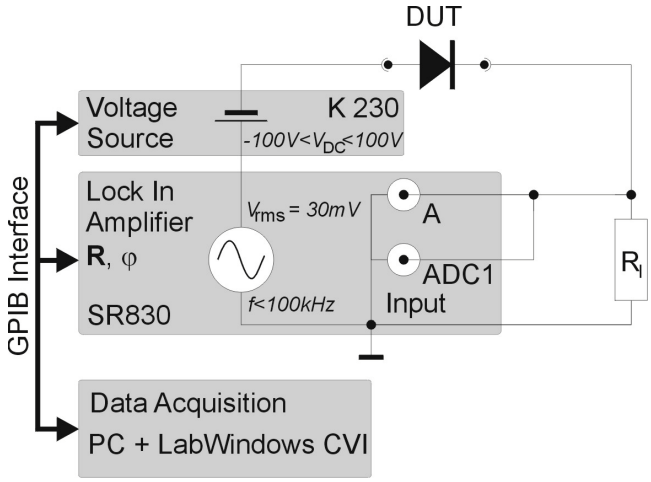

Figure 4. Experimental set up to record C(V) and G_{AC}(V) as a function of the temperature in the dark. The temperature is measured by a Pt100 resistor and directly recorded by ADC inputs of the PC.

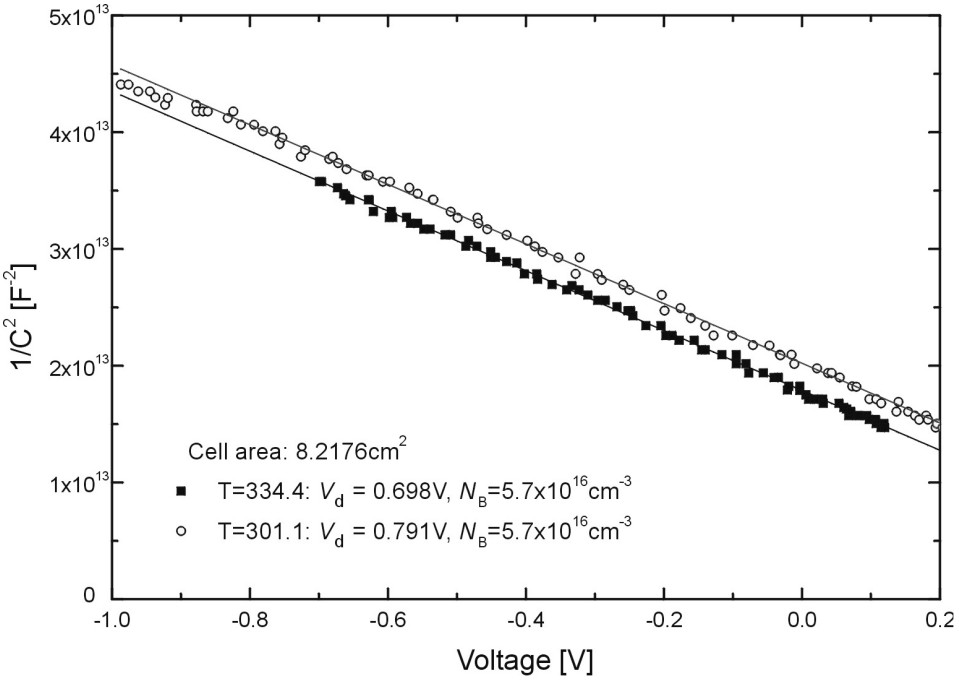

Figure 5. Dependence of the capacitance on the applied DC cell voltage. The linear variation indicates an one sided abrupt planar pn-junction.

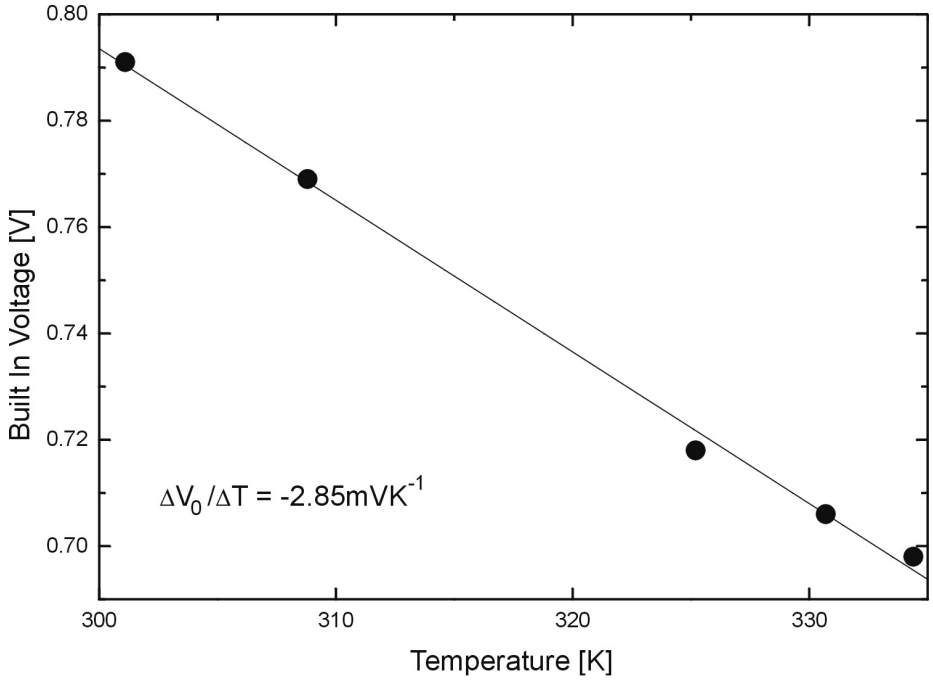

Figure 6. Observed temperature dependence of the built in voltage which was derived from small signal capacitance measurements.

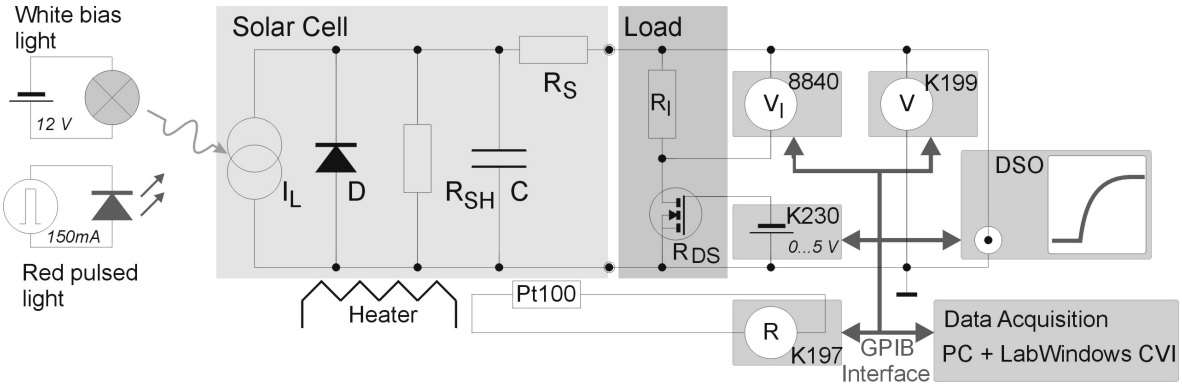

Figure 7. Schematic presentation of the experimental set up used to determine the impedance of the solar cell under illumination. $C=C_T+C_d$, $R_T=R_S+R_I+R_{DS}$, D and R_{SH} determine R_d.

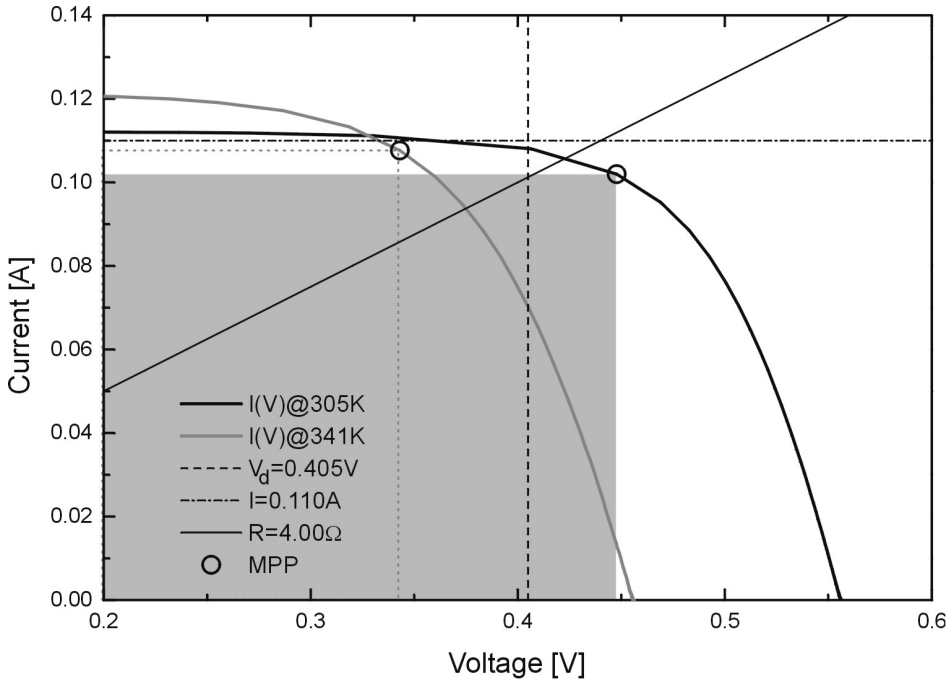

Figure 8. I(V) curve under illumination at two temperatures. Also shown are the lines which indicate the operating conditions of the load resistance during the investigations.

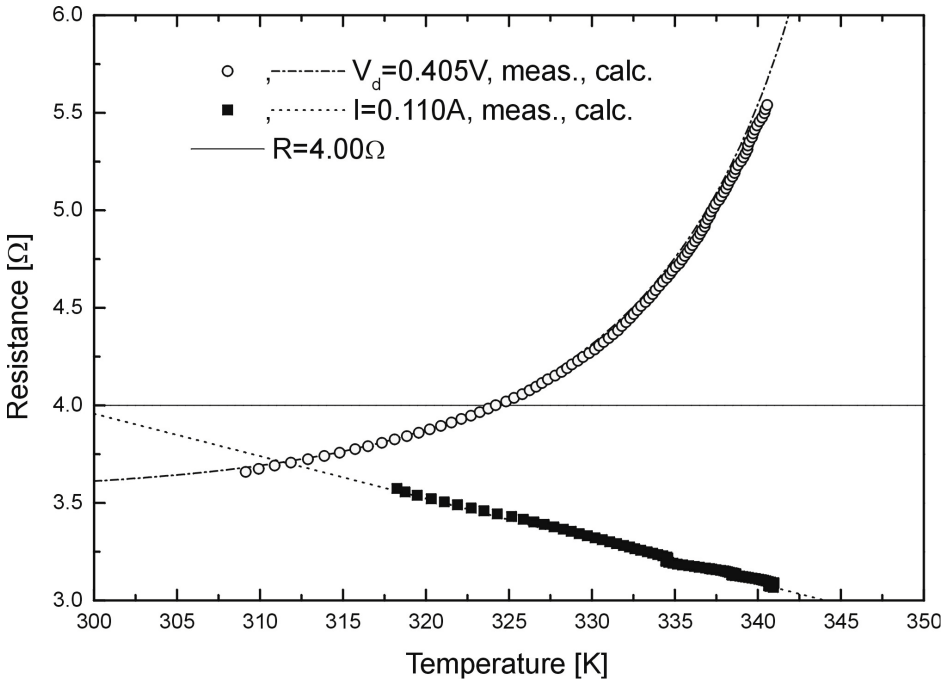

Figure 9. Calculated and measured change of the load resistance with temperature. $R=R_T-R_S$, $R_S=0.26\Omega$=const. for all temperatures

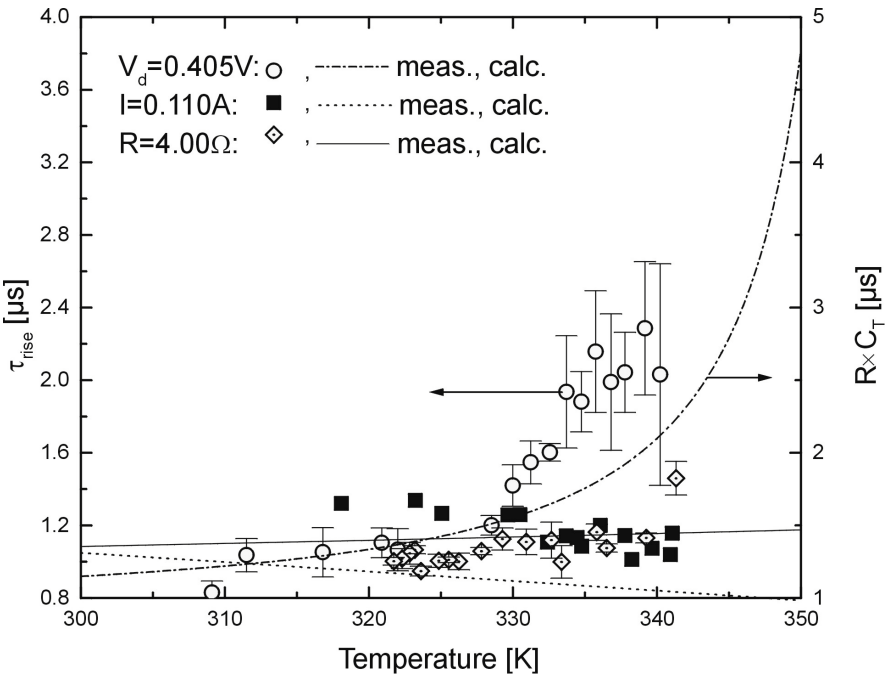

Figure 10. Experimentally determined (Symbols, left axis) and computed values (dashed, dotted and solid line, right axis) of the *RC* time constant as a function of the temperature. C_T are extrapolated values from dark C-V measurements under reverse voltage conditions.

قياس معاملات تيار الخلايا الشمسية السليكونية المتردد

فكتور شلوسر*، أحمد غيطاس+

*معهد فيزياء المواد، كلية الفيزياء، جامعة فيينا، A-1090 فيينا، النمسا
+معمل فيزياء الشمس، المعهد القومي للبحوث الفلكية و الجيوفيزيقية، حلوان، القاهرة، جمهورية مصر العربية

ملخص

إن الوحدات الفوتوفلطية المولدة للكهرباء تعمل بنظام الأجهزة ذو التيار المتردد، و لكنها تُظهر معاوقة كهربائية معقدة و ذلك بسبب تصميم الخلية الشمسية. و لقد صممت العديد من الدوائر الكهربائية لتكييف الطاقة الكهربية من أجل تزويد مقدار الطاقة في حالة التشغيل القياسية.

و لكن أثناء التشغيل، فإن الجزء الحقيقي بالإضافة إلى الجزء التخيلي للمعاوقة الكهربائية للمولدات الفوتوفلطية تتغير بسبب الظروف البيئية المختلفة، مثل تغير شدة الإضاءة و درجة الحرارة. و من ثم فإن أي عدم ملائمة بسبب تغيرات هذه المعاوقة يمكن أن يؤدي إلى انخفاض في أداء نظام توليد الطاقة الكهربائية الكلية. لذلك، لتصميم أنظمة مولدات القوى الفوتوفلطية ذو الكفاءة العالية، فمن الهام القيام بدراسة مفصلة على التيار المتردد للخلايا الشمسية. حيث أن في التطبيقات الأرضية تتعرض الخلية الشمسية لدرجات حرارة متغيرة تتراوح ما بين حوالي 10 إلى 50 درجة مؤية. لذا، لدراسة التأثيرات المحتملة للحرارة على أداء النظام، فأنه يمكن تحديد معاملات التيار المتردد للخلية الشمسية السليكونية مثل السعة الكهربائية و التوصيلية الكهربائية و ذلك عند درجات حرارة مختلفة باستعمال تقنيات مقاييس التيار المتردد للإشارة الصغيرة.

بما أن السعة الانتقالية و التوصيلية للخلية و المحسوبة من مقاييس المعاوقة الكهربائية للإشارة الصغيرة تحت شرط الإظلام فقد لوحظ أن السعة الكهربائية للخلية الشمسية تزيد بينما الجزء الحقيقي لمعاوقة الخلية الكهربائية ينقص بزيادة درجة الحرارة.

من هذه القياسات و تحت الشروط المحددة لتوليد الطاقة الكهربائية فإن المعاوقة الكهربائية المعقدة و المعتمدة على الحرارة قد تم حسابها، بالإضافة إلى أن السعة الكهربائية للخلية الشمسية في حالات التشغيل المختلفة قد تم اشتقاقها من القياسات العابرة تحت شروط الإضاءة. أيضاً، ضمن الخطأ المحدد فإن هذه النتائج أكدت الاختلاف المستنتج للمعاوقة الكهربائية المعقدة مع التغير الحراري.